J Appl Physiol 111: 200–205, 2011.
First published May 12, 2011; doi:10.1152/japplphysiol.00248.2011.

TAT-μUtrophin mitigates the pathophysiology of dystrophin and utrophin double-knockout mice

Jarrod A. Call,[1] James M. Ervasti,[2] and Dawn A. Lowe[1]

[1]*Program in Physical Therapy and Rehabilitation Sciences,* [2]*Department of Biochemistry, Molecular Biology, and Biophysics, University of Minnesota School of Medicine, Minneapolis, Minnesota*

Submitted 24 February 2011; accepted in final form 5 May 2011

Call JA, Ervasti JM, Lowe DA. Tat-μUtrophin mitigates the pathophysiology of dystrophin and utrophin double-knockout mice. *J Appl Physiol* 111: 200–205, 2011. First published May 12, 2011; doi:10.1152/japplphysiol.00248.2011.—Previously, we demonstrated functional substitution of dystrophin by TAT-μUtrophin (TAT-μUtr) in dystrophin-deficient *mdx* mice. Herein, we addressed whether TAT-μUtr could improve the phenotype of dystrophin and utrophin double-knockout (*mdx:utr*$^{-/-}$) mice. Specifically, we quantitatively compared survival and quality of life assessments in *mdx:utr*$^{-/-}$ mice receiving TAT-μUtr protein administration against placebo-treated *mdx:utr*$^{-/-}$ mice (PBS). Additionally, skeletal muscles from TAT-μUtr and PBS mice were tested in vivo and ex vivo for strength and susceptibility to eccentric contraction-induced injury. We found the TAT-μUtr treatment extended life span 45% compared with mice administered PBS. This was attributed to significantly increased food consumption (3.1 vs. 1.8 g/24 h) due to improved ability to search for food as daily cage activities were greater in TAT-μUtr mice (e.g., 364 vs. 201 m ambulation/24 h). The extensor digitorum longus muscles of TAT-μUtr-treated double-knockout mice also displayed increased force-generating capacity ex vivo (8.3 vs. 6.4 N/cm^2) and decreased susceptibility to injury ex vivo and in vivo. These data indicate that the functional benefits of TAT-μUtr replacement treatment extend to the *mdx:utr*$^{-/-}$ double-knockout mouse and support its development as a therapy to mitigate muscle weakness in patients with Duchenne muscular dystrophy.

plantarflexion torque; posterior crural muscles; Duchenne muscular dystrophy

DUCHENNE MUSCULAR DYSTROPHY (DMD) is a progressive muscle wasting disease caused by the loss of the protein dystrophin. Patients with DMD experience precipitous decrements in muscle function with age (23), resulting in wheelchair reliance for mobility by their early teens and ventilator respiratory assistance in their early twenties (18). Muscle function is compromised by the destabilization of the sarcolemma, a result of dystrophin deficiency (2), rendering skeletal muscle susceptible to contraction-induced injury (26). Without a cure, strategies to mitigate the disease progression and improve muscle function have been developed to compensate for dystrophin deficiency by boosting the presence of dystrophin-like cytoskeletal proteins (5, 15, 17, 25). Specifically, utrophin, a protein homologue of dystrophin, sufficiently compensates for dystrophin and improves the phenotype of *mdx* mice, the primary animal model for DMD (11, 28, 30, 33).

Previously, we reported on the efficacy of TAT-μUtrophin (TAT-μUtr) protein administration to boost in vivo levels of utrophin in dystrophic skeletal muscles from *mdx* mice (29). TAT-μUtr is biochemically stable in skeletal muscle and functionally substitutes for dystrophin forming a μUtrophin-glycoprotein complex at the sarcolemma (29). Skeletal muscles from *mdx* mice that received TAT-μUtr presented with a decrease in centrally nucleated fibers, an increase in muscle force, and a diminished susceptibility to contraction-induced injury, indicating TAT-μUtr protein administration mitigates the dystrophic disease in *mdx* mice by reinforcing the sarcolemma. However, given the mild phenotype of the *mdx* mouse compared with patients with DMD, the more clinically relevant mouse model is the dystrophin and utrophin double-knockout mouse (*mdx:utr*$^{-/-}$; 8, 13).

Phenotypically, *mdx:utr*$^{-/-}$ mice are described by a lack of mobility, abnormal gait, abnormal field behavior, joint contractures, severe weight loss, and a shortened life span compared with *mdx* mice (8, 13). Whereas *mdx* mice exhibit an ~25% reduction in skeletal muscle force compared with wild-type mice (22), *mdx:utr*$^{-/-}$ mice exhibit a 60% reduction in peak force (13) and a 38% reduction in skeletal muscle force normalized to muscle cross-sectional area (15). The loss of muscle function in *mdx:utr*$^{-/-}$ mice presumably would contribute to decrements in cage activity, increasing the difficulty to forage for food. Notably, *mdx:utr*$^{-/-}$ mice given a mixture of powdered food and a dish of water on the cage floor were reported to have maintained their body mass for a longer period of time (8). Herein, we sought to determine whether TAT-μUtr protein administration could attenuate these phenotypes in the *mdx:utr*$^{-/-}$ mouse by improving skeletal muscle function.

MATERIALS AND METHODS

TAT-μUtr. TAT-μUtr protein was expressed and purified as previously described (29). Final protein concentrations varied between 4.5 and 9.2 mg/ml.

Mice and study design. The *mdx:utr*$^{-/-}$ mice used in this study were established from *mdx:utr*$^{+/-}$ breeder pairs obtained from Virginia Polytechnic Institute and State University (14) that descended from Washington University (13). Mice were bred and maintained in a specific pathogen-free environment. The genotype of each offspring was determined by PCR analysis of DNA isolated from tail snips as described in detail previously (14). Both male and female mice were used for this study. All mice were given commercial rodent chow and water ad libitum and were housed on a 12-h light/dark cycle. In addition to the food and water provided on cage tops, extra food was placed on the floor of each cage and moistened with water. Cages were changed weekly and moistened food was checked daily for the absence of mold. All protocols and animal care procedures were approved by the University of Minnesota Animal Care and Use Committee.

Two groups of *mdx:utr*$^{-/-}$ mice were used for this study. *Group 1* consisted of 29 *mdx:utr*$^{-/-}$ mice that were assessed only for life span survival. *Group 2* consisted of 22 *mdx:utr*$^{-/-}$ mice used to assess

Address for reprint requests and other correspondence: J. M. Ervasti, Biochemistry, Molecular Biology and Biophysics, Univ. of Minnesota, 6-155 Jackson Hall, 321 Church St. SE, Minneapolis, MN 55455 (e-mail: jervasti@umn.edu).

quality of life (i.e., cage activity and food consumption) and in vivo and ex vivo muscle functions. Within each group, mice received twice weekly intraperitoneal injections of TAT-μUtr at 8.5 μg/g BM (TAT-μUtr; $n = 14$) or equal volume injections of sterilized PBS ($n = 15$) starting at age 14 days (per Ref. 29). All mice were weaned from dams and into individual cages at age 21 days.

Survival. To address whether TAT-μUtr improves the *mdx:utr*$^{-/-}$ mouse phenotype, we determined whether TAT-μUtr prolonged the life span of *mdx:utr*$^{-/-}$ mice. Every morning the health of each mouse was determined by observation either by the primary investigator or a laboratory technician. Time of death was determined by the presence of a carcass on morning inspection or if during the day euthanasia was recommended by a veterinary doctor. The latter occurred twice, and both times mice were found recumbent with a slow heart rate and deep breaths occurring sporadically.

Cage activity assessment. At age 30 days, *mdx:utr*$^{-/-}$ mice were monitored for 24-h cage activities using activity chambers (Med Associates, St. Albans, VT). Infrared arrays in the *x*-, *y*-, and *z*-axes within the activity chambers created a three-dimensional space where cage activity could be monitored by beam breaks. Ambulatory distance was measured by beam breaks occurring in the *x*- and *y*-axis while vertical movements were counted by beam breaks occurring in the *z*-axis. Beam breaks occurring within a 2 × 2-in. area subsequent to the ambulatory cessation for >20 s were counted as stereotypic movements. Direct observation of stereotypic movements can best be described as self-grooming. Active time was calculated by the amount of time during the 24 h that each mouse spent ambulating, jumping, rearing, and grooming.

In addition to monitoring cage activity, food consumption was also measured during the 24-h observational period. Pellets of food, ~6–7 g each, were placed on the floor of the activity cage. The following day the remaining pellet and small particles of food were collected and weighed to determine food consumption per 24 h.

In vivo functional measurements. The plantarflexor contractile performance of the posterior crural muscles (i.e., gastrocnemius, soleus, plantaris muscles) was measured in vivo for TAT-μUtr and PBS mice. We chose to assess hindlimb plantarflexor muscles in vivo for strength and susceptibility to injury because the posterior crural muscles (i.e., gastrocnemius) are more active during ambulation compared with the anterior crural muscles (32). Mice were given a mixture of fentanyl citrate (10 mg/kg BM), droperidol (0.2 mg/kg BM), and diazepam (5 mg/kg BM) and left hindlimbs were shaved and antiseptically prepared by applications of betadine and ethanol. Each mouse was positioned on its right side on a 37°C heated platform with its left foot attached to a machined shoe located on the shaft of a servomotor (model 300B-LR; Aurora Scientific, Aurora, Ontario, Canada). Two platinum electrodes (model E2–12; Grass Technologies, West Warwick, RI) were inserted subcutaneously on either side of the sciatic nerve. To avoid recruitment of the anterior crural muscles responsible for dorsiflexion, the common peroneal nerve was severed. Peak isometric torque was optimized by varying the voltage delivered to the sciatic nerve by the stimulator and stimulus isolation unit (models S48 and SIU5, respectively; Grass Technologies). The parameters for stimulation were set at a 200-ms contraction duration consisting of 0.5-ms square-wave pulses at 150 Hz. Torque as a function of stimulation frequency was then measured during seven isometric contractions at varying stimulation frequencies (20, 40, 60, 80, 100, 125, 150 Hz). Next, the posterior crural muscles were injured by performing 20 eccentric contractions. Muscles were stimulated for 120 ms using the optimal voltage and 150 Hz (16). During stimulation, muscles were stretched from 19° of ankle plantarflexion to 19° of ankle dorsiflexion at an angular velocity of 2000°/s. Eccentric contractions were separated by 10–12 s, and the entire protocol lasted 3.5 min. The selection of a 20 eccentric-contraction protocol was based on preliminary data showing torque loss did not significantly worsen after 20 eccentric contractions. A 5-min rest followed the protocol before maximal isometric torque and torque as a function of stimulation frequency were reassessed. The primary outcome measurements were pre- and post-injury maximal isometric torque and torque-frequency normalized to body mass ($N \cdot mm^{-1} \cdot kg\ BM^{-1}$) and torque loss during the eccentric contraction protocol [i.e., (*eccentric contraction #20* − *eccentric contraction #1*)/*eccentric contraction #1*]. Isometric and eccentric torques reported herein are indicative of the peak isometric and eccentric torques generated during the respective contractions.

Ex vivo contractility. EDL muscles from TAT-μUtr and PBS mice were analyzed ex vivo for force-generating capacities. We chose to assess the hindlimb dorsiflexor EDL muscle ex vivo for contractility and susceptibility to injury for consistency between this and our previous work (29). Mice were anesthetized with pentobarbital sodium (25 mg/kg BM) and muscles were mounted to a dual-mode muscle lever system (300B-LR; Aurora Scientific) and incubated at 25°C in an oxygenated bath as previously described (1, 6, 36). Muscles were maintained at a 0.4 g resting tension (L_o) throughout the experiment (as per 34, 35). Following a 10-min quiescent period, muscles underwent a single passive stretch to 1.05 L_o. Peak twitch force was elicited with a 0.5-ms pulse at 150 V. Maximal isometric tetanic force (P_o) was performed at 150 V and at 180 Hz for 400 ms (Grass S48 stimulator delivered through a SIU5D stimulus isolation unit; Grass Telefactor, Grass Technologies). Active stiffness was determined by applying a sinusoidal length oscillation of 0.01% L_o at 500 Hz at peak force of a single tetanic isometric contraction (12, 31). One minute later, an injury protocol consisting of five eccentric contractions was performed, as per previous work in *mdx:utr*$^{-/-}$ (9, 14) mice and our previous work in *mdx* mice (1, 29). Specifically, muscle were passively shortened to 95% L_o and stimulated for 133 ms while the muscle was simultaneously lengthened to 105% L_o at 0.75 L_o/s, and then passively returned to L_o. Each eccentric contraction was separated by 3 min of rest to avoid fatigue (9, 14, 21). Three minutes after the last eccentric contraction, a final isometric tetanic contraction was performed. Muscle cross-section area was calculated as previously described (3, 34) giving consideration to muscle mass, length, pennation, and density. Maximal isometric and eccentric forces were recorded as the peak isometric and eccentric forces generated during each contraction, respectively. Specific forces (sP_o) were calculated by dividing P_o by muscle cross-sectional area. Eccentric contraction-induced injury was determined by eccentric force loss during the course of the injury protocol [(*contraction #5* − *contraction #1*)/*contraction #1*] and also by the decrement in maximal isometric tetanic force [$(postP_o - P_o)/P_o$].

Muscle mass. Following ex vivo preparations all mice were killed and the tibialis anterior, gastrocnemius, and heart along with extensor digitorum longus muscles, were snap frozen in liquid nitrogen and stored at −80°C. Masses for frozen muscle were later recorded using a microbalance (Sartorius CPA225D; Mettler Toledo, Boston, MA).

Statistics. Survival proportions between TAT-μUtr and PBS mice were statistically analyzed using both Log-Rank and Wilcoxon tests. A Student's *t*-test was used to detect differences between groups concerning cage activities, food consumption, in vivo torque, ex vivo contractility characteristics, and torque and force loss percentages following eccentric contraction-induced injury in vivo and ex vivo, respectively. Data are reported as means ± SE.

RESULTS

The first group of *mdx:utr*$^{-/-}$ mice were injected twice weekly with TAT-μUtr or sterilized PBS. The life span of *mdx:utr*$^{-/-}$ mice receiving injections of TAT-μUtr was 45% longer than mice receiving sterilized PBS (median life span: 43.5 ± 2.0 vs. 30.0 ± 1.8 days, respectively; $P < 0.001$; Fig. 1*A*). Maximal life span was also increased for TAT-μUtr mice (64 vs. 50 days, respectively; $P < 0.001$). Body masses recorded twice weekly during injection showed no significant

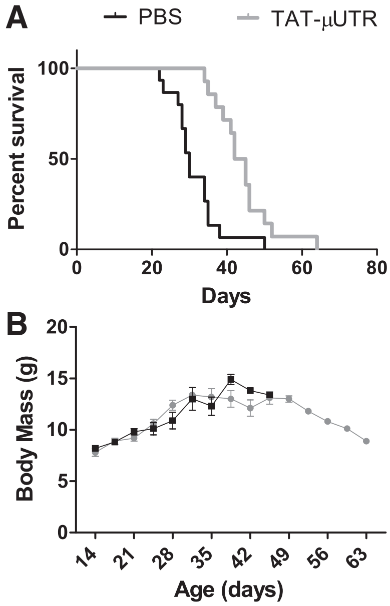

Fig. 1. Effect of TAT-μUtr on survival. *A*: Kaplan-Meier curves. Black bar, PBS, $n = 15$; gray bar, TAT-μUtr, $n = 14$. Survival proportions were extended by ~2 wk with TAT-μUtr treatment; however, treatment did not affect body mass during this time (*B*).

difference between the two groups ($P = 0.517$, Fig. 1*B*). Masses of hindlimb muscles and hearts from TAT-μUtr and PBS mice were analyzed to determine if TAT-μUtr affected muscle size. There were no differences in tibialis anterior, gastrocnemius, EDL, or heart muscle masses between TAT-μUtr and PBS mice for absolute muscle masses ($P \geq 0.280$) or muscle masses normalized to body mass ($P \geq 0.222$).

To investigate factors that may have contributed to an extended life span with TAT-μUtr, we used a second group of *mdx:utr*$^{-/-}$ mice to assess quality of life and muscle function both in vivo and ex vivo.

Quality of life, as measured by food consumption and cage activity, was assessed at age 30 days for both TAT-μUtr and PBS mice. This age was chosen because it corresponded with the median life span of PBS-treated mice from the first group of *mdx:utr*$^{-/-}$ mice.

At age 30 days there was no difference in body masses between TAT-μUtr and PBS mice (12.0 ± 1.0 vs. 10.8 ± 1.0, respectively; $P = 0.371$). However, during the 24-h activity observational period, TAT-μUtr mice consumed 72% more food (3.1 ± 0.3 vs. 1.8 ± 0.2 g/24 h, respectively; $P = 0.002$). We attributed this to a greater ability to search for food because three parameters of cage activity were improved in TAT-μUtr mice compared with PBS mice: ambulatory distance (364 ± 48 vs. 201 ± 22 m/24 h, respectively; $P = 0.004$); stereotypic counts (45.5 ± 2.6 vs. 36.6 ± 33 thousand counts/24 h, respectively; $P = 0.045$); active time (232 ± 18 vs. 178 ± 18 min/24 h, respectively; $P = 0.028$; Fig. 2*A*).

Correlation analyses were performed to determine if cage activities were associated with food consumption. Positive correlations existed between the amount of food consumed and ambulatory distance ($r = 0.5448$; $P = 0.024$), stereotypic activity ($r = 0.6612$; $P < 0.001$), and active time ($r = 0.5765$; $P = 0.015$; Fig. 2, *B–D*).

Maximal isometric in vivo torque was not different between TAT-μUtr and PBS mice (360 ± 20 vs. 340 ± 15 $N \cdot mm^{-1} \cdot kg\ BM^{-1}$, respectively; $P = 0.632$; Fig. 3*A*). Eccentric torque during the injury protocol was reduced ~60% from *eccentric contraction #1* to *eccentric contraction #20* in both groups ($P = 0.805$). TAT-μUtr did affect isometric torque loss following the eccentric injury protocol as TAT-μUtr mice produced 50% more torque compared with PBS mice (166 ± 19 vs. 111 ± 22 $N \cdot mm^{-1} \cdot kg\ BM^{-1}$, respectively; $P = 0.047$; Fig. 3*A*). Isometric torques as a function of stimulation frequency pre- and post-injury are shown in Fig. 3*B*. Consistent with maximal isometric torque, torques elicited at stimulation frequencies 60–150

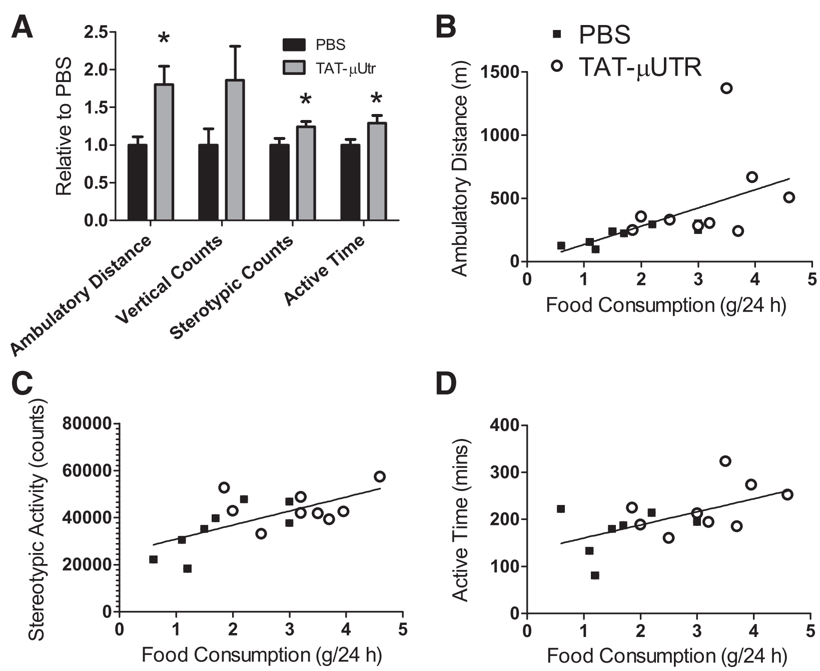

Fig. 2. Effect of TAT-μUtr on cage activities. *A*: ambulatory distance, stereotypic movement, and active time were improved with TAT-μUtr treatment as shown relative to PBS. Additionally, food consumption was positively correlated with ambulatory distance (*B*), stereotypic activity (*C*), and active time (*D*). * > PBS; $P \leq 0.05$.

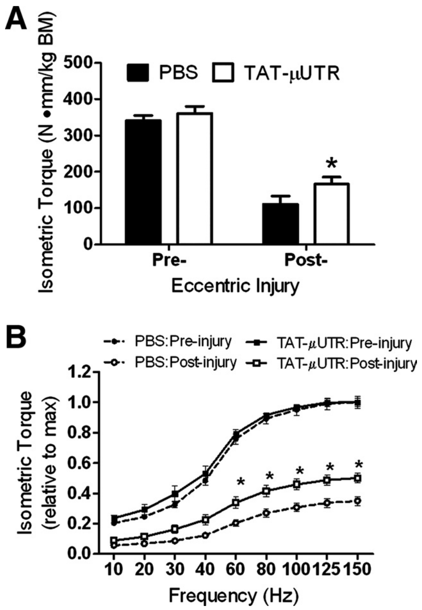

Fig. 3. Effect of TAT-μUtr on in vivo muscle function. *A*: torque loss by the gastrocnemius-soleus-plantaris muscle group following eccentric injury was attenuated with TAT-μUtr treatment. *B*: pre- and post-injury torque-frequency curves shown relative to maximal preinjury torque. * > PBS; $P \leq 0.05$.

Hz assessed postinjury were greater for TAT-μUtr compared with PBS mice ($P \leq 0.032$). These data suggest that muscles from TAT-μUtr-treated mice were less susceptible to eccentric contraction-induced injury.

To determine whether individual muscles from TAT-μUtr-treated mice had better contractility or were less susceptible to eccentric contraction-induced injury, we tested EDL muscles ex vivo. There were no differences between groups in absolute twitch, tetanic, or eccentric forces generated by isolated EDL muscles (Table 1), although there were trends for peak isometric and eccentric forces to be greater in EDL muscle from TAT-μUtr mice ($P = 0.068$ and $P = 0.080$, respectively). However, maximal isometric force normalized to muscle cross-sectional area (i.e., specific tetanic force) was 30% greater in TAT-μUtr mice compared with PBS mice (8.3 ± 1.0 vs. 6.4 ± 0.4 N/cm^2, respectively; $P = 0.026$; Fig. 4*A*). This is an ~15% relative recovery compared with the initial deficit between wild-type and $mdx{:}utr^{-/-}$ mice [wild-type specific force (18.9 ± 1.0 N/cm^2); data not shown]. Specific eccentric force was also 34% greater in TAT-μUtr mice compared with PBS mice (17.0 ± 1.9 vs. 12.7 ± 0.6 N/cm^2, respectively; $P = 0.035$).

Twitch and tetanic force-time tracings were analyzed to determine whether TAT-μUtr affected properties indicative of how fast the EDL muscle contracted and relaxed. There were no differences in these twitch and tetanic parameters between groups (Table 1). Both passive and active stiffness, which reflect the muscle's resistance to lengthening due to noncontractile elastic elements and myosin cross bridges that are strongly bound to actin, respectively, were also not significantly different between groups (Table 1).

There was no effect of TAT-μUtr on EDL muscle force loss during the eccentric injury protocol ($P = 0.385$; Fig. 4*B*), but specific tetanic force following eccentric contraction-induced injury was significantly greater in TAT-μUtr mice compared with PBS mice (4.1 ± 0.6 vs. 2.1 ± 0.3 N/cm^2, respectively; $P = 0.012$; Fig. 4*A*). These data complement the in vivo findings and reinforces that TAT-μUtr mitigates susceptibility to contraction-induced injury.

Table 1. *Ex vivo EDL muscle contractility for TAT-μUtr and PBS mice*

	PBS	TAT-μUtr	*P* value
Mass, mg	3.2 ± 0.4	3.7 ± 0.4	0.448
Length, mm	9.2 ± 0.3	9.7 ± 0.4	0.379
CSA, mm^2	0.72 ± 0.08	0.81 ± 0.07	0.492
Twitch			
P_t, mN	17.8 ± 2.2	22.9 ± 3.2	0.205
TPT, ms	24.1 ± 2.5	31.8 ± 5.5	0.216
$RT_{1/2}$, ms	46.8 ± 6.1	40.1 ± 4.6	0.444
Tetanic			
P_o, mN	47.0 ± 7.2	73.1 ± 11.5	0.068
+dP/d*t*, N/s	1.8 ± 0.3	2.4 ± 0.3	0.220
−dP/d*t*, N/s	−1.0 ± 0.3	−1.8 ± 0.4	0.185
Peak eccentric force, mN	93.1 ± 12.7	137.7 ± 20.6	0.080
Passive stiffness, N/m	23.7 ± 1.4	20.3 ± 2.2	0.225
Active stiffness, N/m	179.5 ± 16.0	223.3 ± 21.0	0.136

Values expressed as means ± SE. P_t, peak twitch force; TPT, time to peak twitch force; $RT_{1/2}$, one-half relaxation time; P_o, maximal isometric tetanic force; +dP/d*t*, maximal rate of tetanic force development; −dP/d*t*; maximal rate of relaxation.

DISCUSSION

Our results show that TAT-μUtr ameliorated the $mdx{:}utr^{-/-}$ mouse phenotype, most notably survival, by increasing skeletal muscle strength and improving activity and food consumption without any increase in body mass. We are not the first to report an improvement in the phenotype of $mdx{:}utr^{-/-}$ mice

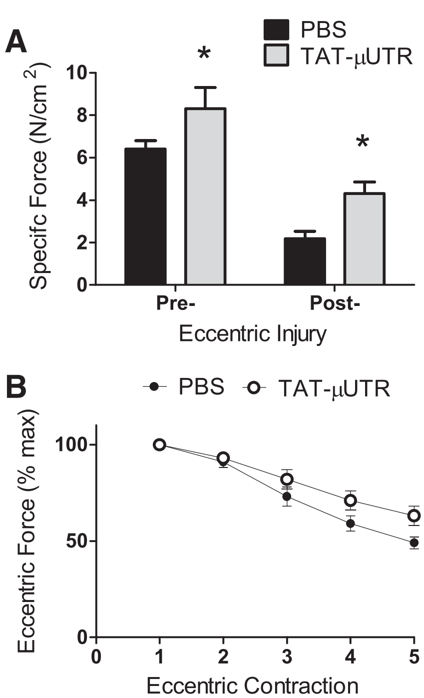

Fig. 4. Effect of TAT-μUtr on ex vivo muscle contractility. *A*: TAT-μUtr improved pre- and post-injury specific tetanic force. *B*: force loss during an eccentric injury protocol was not significantly affected by TAT-μUtr. * > PBS, $P \leq 0.05$.

with μUtrophin or full-length utrophin upregulation (24, 27); however, our findings establish the efficacy of direct protein delivery in improving $mdx:utr^{-/-}$ mice. Here, TAT-μUtr administration affected significant functional and quality of life improvements. We previously demonstrated that TAT-μUtr administration had no effect on expression of full-length utrophin from the endogenous gene (29), suggesting it could be employed in conjunction with other treatment strategies to perhaps achieve additive efficacy.

We chose cage activity as an indication of quality of life and as a quantitative means to characterize the effects of TAT-μUtr and PBS mice. Previously, we showed that wild-type mice were significantly more active than *mdx* mice in terms of ambulatory distance (700 vs. 450 m/24 h) and total active cage time (5.0 vs. 3.5 h/24 h), demonstrating the reliability of cage activity monitoring to quantitatively measure phenotypes (19). Here we detected that TAT-μUtr mice spend 30% more time per day being active and achieved ambulatory distances 81% greater than PBS mice, which approaches ambulation achieved by *mdx* mice (364 vs. 450 m/24 h, TAT-μUtr and *mdx*, respectively). Similar improvements in ambulation (i.e., voluntary wheel running) are observed with μUtrophin upregulation via recombinant adeno-associated viral vectors (24). The increased ability to ambulate through an environment likely affords treated $mdx:utr^{-/-}$ mice the opportunity to find and consume more food, as was shown in our study. The systems most likely affected by μUtrophin therapy that could explain the subsequent increased activity are the skeletal muscle and cardiovascular systems.

Our investigation focused on the function of the posterior crural skeletal muscles in vivo and the EDL muscle ex vivo. To our knowledge we are the first to report in vivo plantarflexion torque capacity for the $mdx:utr^{-/-}$ mouse. Maximal isometric torques are lower in $mdx:utr^{-/-}$ mice compared with *mdx* and wild-type mice (340 vs. 450 and 670 $N \cdot mm^{-1} \cdot kg\ BM^{-1}$, respectively, *mdx* and wild-type values are unpublished). Although preinjury torques were not improved with TAT-μUtr, significantly improved postinjury torques suggest protection of the posterior crural muscles from eccentric contraction-induced injury. This finding was recapitulated ex vivo by greater postinjury EDL specific tetanic force in TAT-μUtr-treated mice. Specific forces reported herein were low compared with previous reports, although EDL force-generating capacity is highly variable for the $mdx:utr^{-/-}$ mouse model (8, 9, 14, 20, 22). Previously, *mdx* mice overexpressing full-length utrophin or injected with TAT-μUtr exhibited marked improvements in EDL muscle force and susceptibility to contraction-induced injury (29, 30, 33). Here we report that similar results were achievable in the $mdx:utr^{-/-}$ mouse with TAT-μUtr and likely contribute to improvements in ambulation.

The culmination of increased muscle function, animal mobility, and food consumption in the $mdx:utr^{-/-}$ mouse appeared to be manifested by extended life span. Previous reports on $mdx:utr^{-/-}$ mouse life span is highly variable, ranging from as little as 4 wk to as many as 36 wk (5, 8, 10, 13, 15, 17, 24). This variability may reflect genetic drift within respective colonies and local environmental factors idiosyncratic to each housing facility (e.g., staff, cage sizes, husbandry, handling, food enrichment options, room noise, architecture, temperature, etc.). While these variables may confound the external validity of certain findings and make inter-laboratory comparisons difficult, it is important to consider these types of various contributing factors. Here, we measured life spans of 7 and 9 wk for $mdx:utr^{-/-}$ mice treated with PBS and TAT-μUtr, respectively, and two factors may have contributed to the relatively short life spans. First, we individually housed each $mdx:utr^{-/-}$ mouse during the life span analysis to ensure consistency of housing from litter to litter. The low body mass and activity of $mdx:utr^{-/-}$ mice impedes the conservation of heat, and individually housed animals were frequently observed shivering. Second, all mice in the study endured twice weekly handling required for IP injections, which likely added stress. Nonetheless, both PBS and TAT-μUtr mice were handled identically and we observed an improvement in life span of the mice that received TAT-μUtr treatments.

Loss of muscle function is a well-established consequence of dystrophin deficiency (4, 7, 8, 13). Herein, we observed modest, but significant improvements in skeletal muscle function and life span of TAT-μUtr mice. We conclude TAT-μUtr may be a viable treatment strategy for patients with DMD; however, investigation into its effectiveness in combination with other therapies as well as its effects on muscle recovery and adaptation are warranted.

GRANTS

This study was supported by grants from the Muscular Dystrophy Association, The Nash Avery Foundation, Charley's Fund, and the National Institutes of Health (P30-AR-05722, T32-AR-07612, and KO2-AG036827).

DISCLOSURES

J. M. Ervasti is a coinventor on US Patent No. 7,863,017: TAT-Utrophin as a Protein Therapy for Dystrophinopathies.

REFERENCES

1. **Baltgalvis KA, Call JA, Nikas JB, Lowe DA.** Effects of prednisolone on skeletal muscle contractility in mdx mice. *Muscle Nerve* 40: 443–454, 2009.
2. **Blake DJ, Weir A, Newey SE, Davies KE.** Function and genetics of dystrophin and dystrophin-related proteins in muscle. *Physiol Rev* 82: 291–329, 2002.
3. **Brooks SV, Faulkner JA.** Contractile properties of skeletal muscles from young, adult and aged mice. *J Physiol* 404: 71–82, 1988.
4. **Bulfield G, Siller WG, Wight PA, Moore KJ.** X chromosome-linked muscular dystrophy (mdx) in the mouse. *Proc Natl Acad Sci USA* 81: 1189–1192, 1984.
5. **Burkin DJ, Wallace GQ, Nicol KJ, Kaufman DJ, Kaufman SJ.** Enhanced expression of the alpha 7 beta 1 integrin reduces muscular dystrophy and restores viability in dystrophic mice. *J Cell Biol* 152: 1207–1218, 2001.
6. **Call JA, McKeehen JN, Novotny SA, Lowe DA.** Progressive resistance voluntary wheel running in the *mdx* mouse. *Muscle Nerve* 42: 871–880, 2010.
7. **Cooper BJ, Winand NJ, Stedman H, Valentine BA, Hoffman EP, Kunkel LM, Scott MO, Fischbeck KH, Kornegay JN, Avery RJ, Williams JR, Schmickel RD, Sylvester JE.** The homologue of the Duchenne locus is defective in X-linked muscular dystrophy of dogs. *Nature* 334: 154–156, 1988.
8. **Deconinck AE, Rafael JA, Skinner JA, Brown SC, Potter AC, Metzinger L, Watt DJ, Dickson JG, Tinsley JM, Davies KE.** Utrophin-dystrophin-deficient mice as a model for Duchenne muscular dystrophy. *Cell* 90: 717–727, 1997.
9. **Deconinck N, Rafael JA, Beckers-Bleukx G, Kahn D, Deconinck AE, Davies KE, Gillis JM.** Consequences of the combined deficiency in dystrophin and utrophin on the mechanical properties and myosin composition of some limb and respiratory muscles of the mouse. *Neuromuscul Disord* 8: 362–370, 1998.
10. **Gaedigk R, Law DJ, Fitzgerald-Gustafson KM, McNulty SG, Nsumu NN, Modrcin AC, Rinaldi RJ, Pinson D, Fowler SC, Bilgen M, Burns**

J, Hauschka SD, White RA. Improvement in survival and muscle function in an mdx/utrn(−/−) double mutant mouse using a human retinal dystrophin transgene. *Neuromuscul Disord* 16: 192–203, 2006.
11. **Gilbert R, Nalbantoglu J, Petrof BJ, Ebihara S, Guibinga GH, Tinsley JM, Kamen A, Massie B, Davies KE, Karpati G.** Adenovirus-mediated utrophin gene transfer mitigates the dystrophic phenotype of mdx mouse muscles. *Hum Gene Ther* 10: 1299–1310, 1999.
12. **Gordon T, Stein RB.** Comparison of force and stiffness in normal and dystrophic mouse muscles. *Muscle Nerve* 11: 819–827, 1988.
13. **Grady RM, Teng H, Nichol MC, Cunningham JC, Wilkinson RS, Sanes JR.** Skeletal and cardiac myopathies in mice lacking utrophin and dystrophin: a model for Duchenne muscular dystrophy. *Cell* 90: 729–738, 1997.
14. **Grange RW, Gainer TG, Marschner KM, Talmadge RJ, Stull JT.** Fast-twitch skeletal muscles of dystrophic mouse pups are resistant to injury from acute mechanical stress. *Am J Physiol Cell Physiol* 283: C1090–C1101, 2002.
15. **Gregorevic P, Allen JM, Minami E, Blankinship MJ, Haraguchi M, Meuse L, Finn E, Adams ME, Froehner SC, Murry CE, Chamberlain JS.** rAAV6-microdystrophin preserves muscle function and extends lifespan in severely dystrophic mice. *Nat Med* 12: 787–789, 2006.
16. **Ingalls CP, Warren GL, Lowe DA, Boorstein DB, Armstrong RB.** Differential effects of anesthetics on in vivo skeletal muscle contractile function in the mouse. *J Appl Physiol* 80: 332–340, 1996.
17. **Kawano R, Ishizaki M, Maeda Y, Uchida Y, Kimura E, Uchino M.** Transduction of full-length dystrophin to multiple skeletal muscles improves motor performance and life span in utrophin/dystrophin double knockout mice. *Mol Ther* 16: 825–831, 2008.
18. **Kohler M, Clarenbach CF, Bahler C, Brack T, Russi EW, Bloch KE.** Disability and survival in Duchenne muscular dystrophy. *J Neurol Neurosurg Psychiatry* 80: 320–325, 2009.
19. **Landisch RM, Kosir AM, Nelson SA, Baltgalvis KA, Lowe DA.** Adaptive and nonadaptive responses to voluntary wheel running by mdx mice. *Muscle Nerve* 38: 1290–1303, 2008.
20. **Li D, Yue Y, Duan D.** Marginal level dystrophin expression improves clinical outcome in a strain of dystrophin/utrophin double knockout mice. *PLoS One* 5: e15286.
21. **Lowe DA, Warren GL, Hayes DA, Farmer MA, Armstrong RB.** Eccentric contraction-induced injury of mouse soleus muscle: effect of varying $[Ca^{2+}]_o$. *J Appl Physiol* 76: 1445–1453, 1994.
22. **Lowe DA, Williams BO, Thomas DD, Grange RW.** Molecular and cellular contractile dysfunction of dystrophic muscle from young mice. *Muscle Nerve* 34: 92–100, 2006.
23. **Mattar FL, Sobreira C.** Hand weakness in Duchenne muscular dystrophy and its relation to physical disability. *Neuromuscul Disord* 18: 193–198, 2008.
24. **Odom GL, Gregorevic P, Allen JM, Finn E, Chamberlain JS.** Microutrophin delivery through rAAV6 increases lifespan and improves muscle function in dystrophic dystrophin/utrophin-deficient mice. *Mol Ther* 16: 1539–1545, 2008.
25. **Peter AK, Marshall JL, Crosbie RH.** Sarcospan reduces dystrophic pathology: stabilization of the utrophin-glycoprotein complex. *J Cell Biol* 183: 419–427, 2008.
26. **Petrof BJ, Shrager JB, Stedman HH, Kelly AM, Sweeney HL.** Dystrophin protects the sarcolemma from stresses developed during muscle contraction. *Proc Natl Acad Sci USA* 90: 3710–3714, 1993.
27. **Rafael JA, Tinsley JM, Potter AC, Deconinck AE, Davies KE.** Skeletal muscle-specific expression of a utrophin transgene rescues utrophin-dystrophin deficient mice. *Nat Genet* 19: 79–82, 1998.
28. **Rybakova IN, Patel JR, Davies KE, Yurchenco PD, Ervasti JM.** Utrophin binds laterally along actin filaments and can couple costameric actin with sarcolemma when overexpressed in dystrophin-deficient muscle. *Mol Biol Cell* 13: 1512–1521, 2002.
29. **Sonnemann KJ, Heun-Johnson H, Turner AJ, Baltgalvis KA, Lowe DA, Ervasti JM.** Functional substitution by TAT-utrophin in dystrophin-deficient mice. *PLoS Med* 6: e1000083, 2009.
30. **Squire S, Raymackers JM, Vandebrouck C, Potter A, Tinsley J, Fisher R, Gillis JM, Davies KE.** Prevention of pathology in mdx mice by expression of utrophin: analysis using an inducible transgenic expression system. *Hum Mol Genet* 11: 3333–3344, 2002.
31. **Stein RB, Gordon T.** Nonlinear stiffness—force relationships in whole mammalian skeletal muscles. *Can J Physiol Pharmacol* 64: 1236–1244, 1986.
32. **Thota AK, Watson SC, Knapp E, Thompson B, Jung R.** Neuromechanical control of locomotion in the rat. *J Neurotrauma* 22: 442–465, 2005.
33. **Tinsley J, Deconinck N, Fisher R, Kahn D, Phelps S, Gillis JM, Davies K.** Expression of full-length utrophin prevents muscular dystrophy in mdx mice. *Nat Med* 4: 1441–1444, 1998.
34. **Warren GL, Hayes DA, Lowe DA, Williams JH, Armstrong RB.** Eccentric contraction-induced injury in normal and hindlimb-suspended mouse soleus and EDL muscles. *J Appl Physiol* 77: 1421–1430, 1994.
35. **Warren GL, Ingalls CP, Armstrong RB.** Temperature dependency of force loss and Ca(2+) homeostasis in mouse EDL muscle after eccentric contractions. *Am J Physiol Regul Integr Comp Physiol* 282: R1122–R1132, 2002.
36. **Warren GL, Moran AL, Hogan HA, Lin AS, Guldberg RE, Lowe DA.** Voluntary run training but not estradiol deficiency alters the tibial bone-soleus muscle functional relationship in mice. *Am J Physiol Regul Integr Comp Physiol* 293: R2015–R2026, 2007.